INTERNATIONAL JOURNAL FOR NUMERICAL METHODS IN FLUIDS, VOL. 4, 109–125 (1984)

A METHOD FOR SOLVING THE FACTORIZED VORTICITY–STREAM FUNCTION EQUATIONS BY FINITE ELEMENTS

L. QUARTAPELLE

Istituto di Fisica, Politecnico di Milano, Piazza Leonardo da Vinci 32, 20133, Milano, Italy

AND

M. NAPOLITANO

Istituto di Macchine, Università di Bari, Italy

SUMMARY

A new finite element method for solving the time-dependent incompressible Navier–Stokes equations with general boundary conditions is presented. The two second-order partial differential equations for the vorticity and the stream function are factorized, apart from the non-linear advection term, by eliminating the coupling due to the double specification on the stream function at (a part of) the boundary. This is achieved by reducing the no-slip boundary conditions to projection integral conditions for the vorticity field and by evaluating the relevant quantities involved according to an extension of the method of Glowinski and Pironneau for the biharmonic problem. Time integration schemes and iterative algorithms are introduced which require the solution only of banded linear systems of symmetric type. The proposed finite element formulation is compared with its finite difference equivalent by means of a few numerical examples. The results obtained using 4-noded bilinear elements provide an illustration of the superiority of the finite element based spatial discretization.

KEY WORDS Finite elements Navier–Stokes Vorticity–stream function Time-dependent flows Boundary conditions Incompressible viscous flows Two-dimensional flows

INTRODUCTION

A major difficulty in the numerical solution of the Navier–Stokes equations in terms of the vorticity and stream function variables is due to the absence of boundary conditions for the vorticity. In fact, the specification of the velocity at the boundary translates into boundary conditions for the stream function and its normal derivative. This introduces a coupling between the vorticity and stream function equations which is additional to the one coming from the non-linear advection term in the vorticity transport equation. Therefore, even in the linear case of Stokes' flows, one is faced with the problem of solving a system of two second-order partial differential equations, which is essentially a single fourth-order partial differential equation. Such a difficulty can be circumvented when the vorticity and stream function equations are solved via the finite difference method (FDM), in so far as this discretization procedure is well suited either to a direct imposition of the two boundary conditions for the stream function[1] or to an iterative evaluation of the vorticity at the

0271–2091/84/020109–17$01.70

Received 5 July 1982
Revised 21 October 1982

boundary[2–4] and this is probably the reason why most numerical solutions of the vorticity–stream function equations still employ finite differences.

On the other hand, in the finite element method (FEM) the absence of essential or natural boundary conditions for the vorticity poses in general greater difficulties to the numerical analyst. (For an attempt at employing the FD artifices in an FE context see Reference 5). In fact, in order to establish appropriate finite element equations, special interpolation polynomials, assuring the continuity of the stream function first derivatives at interelement boundaries, have to be used, consistent with the effective fourth-order character of the differential problem. The resulting procedure, although feasible and clearly implemented,[6,7] is certainly much more cumbersome than the one relying on the solution of second-order equations. Other finite element researchers have eliminated the aforementioned difficulty by using a mixed approach,[8–11] which requires neither boundary conditions for the vorticity nor higher-order continuity of the stream function interpolation. However, the resulting system of algebraic equations contains all the nodal values of both the stream function and the vorticity as unknowns and it may soon become too large to be handled when a fine resolution is sought. It is for these reasons that the finite element method, more than the finite difference method, can benefit from the availability of integral conditions for the vorticity and of the consequent split formulation of the vorticity and stream function equations.[12–14] For the case of steady-state creeping flows, Glowinski and Pironneau[15] have developed a clean finite element method to solve directly the biharmonic equation, essentially as a system of two Poisson equations, each being supplemented by its own conditions of integral and boundary type, respectively. The extension of such an approach to the complete time-dependent non-linear equations being not available to date, it appears very worthwhile to provide a finite element formulation which takes full advantage of the integral conditions for the vorticity and is capable of dealing with boundary conditions of general type, as done in the present paper.

The Navier–Stokes equations are written in a weak form together with the integral vorticity conditions. A simple two-level finite difference scheme is used for the time discretization focusing the attention on the most effective way of solving possibly non-symmetric and non-linear finite element equations. A single general algorithm for the solution of the aforementioned equations is presented which consists of an iterative procedure dealing only with banded linear systems of symmetric type. The validity and potentiality of the proposed approach is demonstrated by means of a few numerical tests. The results obtained using isoparametric 4-noded quadrilateral elements compare favourably with the finite difference results obtained on a twice finer mesh.

VORTICITY–STREAM FUNCTION EQUATIONS WITH GENERAL BOUNDARY CONDITIONS

Let Ω be a simply connected bounded domain of the plane with a smooth boundary Γ. The two-dimensional motion of a viscous incompressible fluid can be described in terms of the vorticity and stream function variables, ζ and ψ, by the dimensionless time-dependent Navier–stokes equations

$$-\nabla^2\zeta/Re+\frac{\partial\zeta}{\partial t}+J(\zeta,\psi)=0 \tag{1}$$

$$-\nabla^2\psi=\zeta \tag{2}$$

Table I

Γ_0	Γ_1	Γ_2	Γ_3	Γ_4
$\frac{\partial\psi}{\partial n}=b_0$	$\zeta=c$	$\frac{\partial\zeta}{\partial n}=d$	$\zeta=c$	$\frac{\partial\zeta}{\partial n}=d$
$\psi=a$			$\frac{\partial\psi}{\partial n}=b$	

where Re is the Reynolds number and $J(\zeta, \psi)\equiv\partial(\zeta, \psi)/\partial(x, y)$ is the Jacobian. We denote by Γ_l, $l=0, 1, \ldots, 4$, the parts of Γ on which different boundary conditions are prescribed: Γ_0 is characterized by two conditions for the variable ψ, whereas the remaining parts Γ_l, $l>0$, allow for all combinations of Dirichlet and Neumann boundary conditions for ζ and ψ, as indicated in Table I.

We denote by $\Gamma_{D\zeta}$ and $\Gamma_{N\zeta}$ (resp. $\Gamma_{D\psi}$ and $\Gamma_{N\psi}$) the portions of Γ at which Dirichlet and Neumann conditions are prescribed for ζ (resp. ψ), namely,

$$\Gamma_{D\zeta}=\Gamma_1\cup\Gamma_3, \qquad \Gamma_{N\zeta}=\Gamma_2\cup\Gamma_4$$
$$\Gamma_{D\psi}=\Gamma_0\cup\Gamma_1\cup\Gamma_2, \qquad \Gamma_{N\psi}=\Gamma_3\cup\Gamma_4$$

Notice that, since there is a double specification for ψ on Γ_0, $\Gamma_0\not\subset\Gamma_{N\psi}$ and $\Gamma=\Gamma_0\cup\Gamma_{D\zeta}\cup\Gamma_{N\zeta}=\Gamma_{D\psi}\cup\Gamma_{N\psi}$. We point out that all the aforementioned conditions are considered for the sake of generality, even though the crucial point in order to formulate the Navier–Stokes equations in split form is to transform the Neumann boundary conditions for ψ on Γ_0 (where a Dirichlet boundary condition for ψ is also prescribed) into an independent conditioning for the vorticity. Such vorticity conditions turn out bo be of an integral character, as demonstrated by the following theorem.

Theorem

$$\zeta=-\nabla^2\psi, \quad \text{with} \quad \psi|_{\Gamma_{D\psi}}=a, \qquad \left.\frac{\partial\psi}{\partial n}\right|_{\Gamma_{N\psi}}=b(\Gamma_{D\psi}\cup\Gamma_{N\psi}=\Gamma) \quad \text{and} \quad \left.\frac{\partial\psi}{\partial n}\right|_{\Gamma_0}=b_0\,(\Gamma_0\subseteq\Gamma_{D\psi}),$$

if and only if

$$\int_\Omega \zeta\eta=-\int_{\Gamma_0} b_0\eta-\int_{\Gamma_{N\psi}} b\eta+\int_{\Gamma_{D\psi}} a\frac{\partial\eta}{\partial n} \tag{3}$$

for any harmonic function η which is the solution of the problem: for each $s\in\Gamma_0$ find η such that

$$\nabla^2\eta=0 \tag{4a}$$
$$\eta|_{\Gamma_0}=\delta(\tilde{s}-s), \qquad \tilde{s}\in\Gamma_0 \tag{4b}$$
$$\eta|_{\Gamma_{D\psi}\setminus\Gamma_0}=0 \tag{4c}$$
$$\left.\frac{\partial\eta}{\partial n}\right|_{\Gamma_{N\psi}}=0 \tag{4d}$$

This theorem can be proven by means of Green's formula much in the same manner as the

theorem given by Quartapelle and Valz-Gris.[13] By virtue of the integral vorticity conditions (3), equations (1) and (2) can be split, as far as the respective conditioning is concerned, into the following form

$$-\nabla^2\zeta/Re+\frac{\partial\zeta}{\partial t}+J(\zeta,\psi)=0 \tag{5a}$$

$$\int_\Omega \zeta\eta=-\int_{\Gamma_0} b_0\eta-\int_{\Gamma_{N\psi}} b\eta+\int_{\Gamma_{D\psi}} a\frac{\partial\eta}{\partial n} \tag{5b}$$

$$\zeta|_{\Gamma_{D\zeta}}=c,\qquad \left.\frac{\partial\zeta}{\partial n}\right|_{\Gamma_{N\zeta}}=d \tag{5c}$$

$$-\nabla^2\psi=\zeta \tag{6a}$$

$$\psi|_{\Gamma_{D\psi}}=a,\qquad \left.\frac{\partial\psi}{\partial n}\right|_{\Gamma_{N\psi}}=b \tag{6b}$$

where η is any harmonic function defined by problem (4).

TIME-DISCRETIZED EQUATIONS AND ALGORITHMS

Starting from equations (5) and (6), discrete approximations and numerical algorithms for the calculation of steady and unsteady flows can be derived. For simplicity, we use a two-level finite difference time discretization, as follows:

$$(-\nabla^2+e)\zeta^{n+1}+Re\,J(\zeta^r,\psi^s)=e\zeta^n \tag{7a}$$

$$\int_\Omega \zeta^{n+1}\eta=-\int_{\Gamma_0} b_0^{n+1}\eta-\int_{\Gamma_{N\psi}} b^{n+1}\eta+\int_{\Gamma_{D\psi}} a^{n+1}\frac{\partial\eta}{\partial n} \tag{7b}$$

$$\zeta^{n+1}|_{\Gamma_{D\zeta}}=c^{n+1},\qquad \left.\frac{\partial\zeta^{n+1}}{\partial n}\right|_{\Gamma_{N\zeta}}=d^{n+1} \tag{7c}$$

$$-\nabla\psi^{n+1}=\zeta^{n+1} \tag{8a}$$

$$\psi^{n+1}|_{\Gamma_{D\psi}}=a^{n+1},\qquad \left.\frac{\partial\psi^{n+1}}{\partial n}\right|_{\Gamma_{N\psi}}=b^{n+1} \tag{8b}$$

where $e\equiv Re/\Delta t$, $a^{n+1}=a(t^{n+1})$ and similarly for b, b_0, c, d. An implicit treatment of the linear part has been assumed, whereas the non-linear advection part is taken into account with an increasing degree of implicitness, depending on the values chosen for r and s: we have four possible schemes.[14]

Explicit scheme: $r=s=n$

The Helmholtz equation (7a) for ζ^{n+1} is supplemented by the integral conditions (7b) and boundary conditions of Dirichlet and Neumann type (7c). This equation is independent of the Poisson equation (8a) for ψ^{n+1} which is supplemented by boundary conditions (8b). The two equations can be solved in sequence but the value of time step Δt will be restricted by stability conditions.

ζ-implicit scheme: $r=n+1$, $s=n$

The vorticity equation is still uncoupled from the Poisson equation for the stream function but now, owing to the term $J(\zeta^{n+1},\psi^n)$, it contains a non-symmetric and non-constant part

which is different at each time level. The two equations can still be solved in sequence. The scheme is (linearly) implicit and therefore it will be unconditionally stable except for possible non-linear effects.

ψ-implicit scheme: $r = n$, $s = n+1$

The vorticity and stream function equations are now coupled linearly through the term $J(\zeta^n, \psi^{n+1})$ and therefore they must be solved altogether. As far as the numerical stability is concerned, the ψ-implicit scheme has properties similar to the ζ-implicit scheme.

Implicit scheme: $r = s = n+1$

In this case the equations are coupled together non-linearly through the advection term $J(\zeta^{n+1}, \psi^{n+1})$ and an iterative method of solution is required. The time integration scheme is unconditionally stable even with respect to non-linear instabilities.

In order to solve the non-linear equations of the implicit scheme, we use an iterative algorithm which deals only with symmetric equations independent of the time level. For computational convenience such an algorithm is also used for solving the non-symmetric advective part of the linear equations of the ζ- and ψ-implicit schemes, iteratively. The solution $(\zeta, \psi)^{n+1}$ is obtained as the limit of the sequence $(\zeta, \psi)^m$, $m = 0, 1, \ldots$, calculated as follows. Start from $(\zeta, \psi)^{m=0} = (\zeta, \psi)^n$. Then, from ζ^n, $(a, b, b_0, c, d)^{n+1}$ and $(\zeta, \psi)^m$, determine ζ^{m+1} and ψ^{m+1} as the solutions of the equations

$$(-\nabla^2 + e)\zeta^{m+1} = e\zeta^n - Re\, J(\zeta^p, \psi^q) \tag{9a}$$

$$\int_\Omega \zeta^{m+1}\eta = -\int_{\Gamma_0} b_0^{n+1}\eta - \int_{\Gamma_{N\psi}} b^{n+1}\eta + \int_{\Gamma_{D\psi}} a^{n+1}\frac{\partial \eta}{\partial n} \tag{9b}$$

$$\zeta^{m+1}|_{\Gamma_{D\zeta}} = c^{n+1}, \qquad \left.\frac{\partial \zeta^{m+1}}{\partial n}\right|_{\Gamma_{N\zeta}} = d^{n+1} \tag{9c}$$

$$-\nabla^2 \psi^{m+1} = \zeta^{m+1} \tag{9d}$$

$$\psi^{m+1}|_{\Gamma_{D\psi}} = a^{n+1}, \qquad \left.\frac{\partial \psi^{m+1}}{\partial n}\right|_{\Gamma_{N\psi}} = b^{n+1}. \tag{9e}$$

The iterative process is terminated when

$$\|(\zeta, \psi)^{m+1} - (\zeta, \psi)^m\| \leqslant \varepsilon$$

for some norm and a small positive constant ε. According to the values chosen for p and q in the vorticity equation (9a), such an algorithm solves the equations of the three different schemes:

$p = m, q = n$: the iteration defined by equations (9a)–(9c) solves the vorticity equation of the ζ-implicit scheme

$p = n, q = m$: the iteration defined by equations (9) solves the linear system of the two coupled equations of the ψ-implicit scheme

$p = m, q = m$: the iteration (9) solves the non-linear system of the two equations of the implicit scheme.

VORTICITY EQUATION WITH MIXED INTEGRAL AND BOUNDARY CONDITIONS

The vorticity equations to be solved in all of the present schemes have the typical form

$$(-\nabla^2 + e)\zeta = f \tag{10a}$$

$$\int_\Omega \zeta\eta = -\int_{\Gamma_0} b_0\eta - \int_{\Gamma_{N\psi}} b\eta + \int_{\Gamma_{D\psi}} a\frac{\partial\eta}{\partial n} \tag{10b}$$

$$\zeta|_{\Gamma_{D\zeta}} = c, \qquad \left.\frac{\partial\zeta}{\partial n}\right|_{\Gamma_{N\zeta}} = d \tag{10c}$$

where ζ is the unknown and $f = e\zeta^n - Re\,J(\zeta^p, \psi^q)$ is known. In order to solve the linear problem (10) we use the following decomposition scheme. The solution is written in the form

$$\zeta = \bar{\zeta} + \sum \lambda\zeta', \tag{11}$$

where, for each $s' \in \Gamma_0$, ζ' is the solution of the homogeneous problem

$$(-\nabla^2 + e)\zeta' = 0 \tag{12a}$$

$$\zeta'|_{\Gamma_0} = \delta(s - s'),\ s \in \Gamma_0, \qquad \zeta'|_{\Gamma_{D\zeta}} = 0, \qquad \left.\frac{\partial\zeta'}{\partial n}\right|_{\Gamma_{N\zeta}} = 0, \tag{12b}$$

and $\bar{\zeta}$ is the solution of the non-homogeneous problem

$$(-\nabla^2 + e)\bar{\zeta} = f \tag{13a}$$

$$\bar{\zeta}|_{\Gamma_0} = \text{arbitrary}, \qquad \bar{\zeta}|_{\Gamma_{D\zeta}} = c, \qquad \left.\frac{\partial\bar{\zeta}}{\partial n}\right|_{\Gamma_{N\zeta}} = d \tag{13b}$$

By imposing that the vorticity ζ satisfies the integral conditions (10b), we obtain the following linear problem for the unknown λ

$$A\lambda = \beta \tag{14}$$

where A and β are defined by

$$A(s, s') = \int_\Omega \zeta'\eta \tag{15}$$

and

$$\beta(s) = -\int_\Omega \bar{\zeta}\eta - \int_{\Gamma_0} b_0\eta - \int_{\Gamma_{N\psi}} b\eta + \int_{\Gamma_{D\psi}} a\frac{\partial\eta}{\partial n} \tag{16}$$

respectively. By means of Green's formula, it is possible to show that the operator A is symmetric. We notice in passing that this decomposition scheme can be regarded, in the spatially discretized case, as a block Gaussian elimination exploiting the special structure of the linear system of the algebraic equations (10).

GLOWINSKI–PIRONNEAU METHOD

The evaluation of A and β directly from equations (15) and (16) is computationally not convenient since in these expressions explicit reference is made to the harmonic functions η. Glowinski and Pironneau have demonstrated for the biharmonic equation[15] that A and β

can also be characterized equivalently without any reference to η at the expense of doubling the number of elliptic equations to be solved. Their method is extended here to the case of the time-dependent equations supplement by general boundary conditions. In place of the harmonic functions η defined by problem (4), for each $s \in \Gamma_0$ a function is introduced which satisfies the same boundary conditions (4b)–(4d) but is otherwise arbitrary in Ω, i.e.

$$w = \text{arbitrary in } \Omega \tag{17a}$$

$$w|_{\Gamma_0} = \delta(\tilde{s} - s), \qquad \tilde{s} \in \Gamma_0 \tag{17b}$$

$$w|_{\Gamma_{D\psi} \setminus \Gamma_0} = 0 \tag{17c}$$

$$\left.\frac{\partial w}{\partial n}\right|_{\Gamma_{N\psi}} = 0 \tag{17d}$$

Then, for each $s' \in \Gamma_0$ the following two elliptic problems for ζ' and ψ' are solved in sequence

$$(-\nabla^2 + e)\zeta' = 0 \tag{18a}$$

$$\zeta'|_{\Gamma_0} = w'|_{\Gamma_0}, \qquad \zeta'|_{\Gamma_{D\zeta}} = 0, \qquad \left.\frac{\partial \zeta'}{\partial n}\right|_{\Gamma_{N\zeta}} = 0 \tag{18b}$$

and

$$-\nabla^2 \psi' = \zeta' \tag{19a}$$

$$\psi'|_{\Gamma_0} = 0 \qquad \left.\frac{\partial \psi'}{\partial n}\right|_{\Gamma_{N\psi}} = 0 \tag{19b}$$

By virtue of Green's formula, it can be shown that equation (15) implies that

$$A(s, s') = \int_\Omega (\zeta' w - \nabla \psi' \cdot \nabla w) \tag{20}$$

In a similar way, the two following equations for $\bar{\zeta}$ and $\bar{\psi}$ are solved

$$(-\nabla^2 + e)\bar{\zeta} = f \tag{21a}$$

$$\bar{\zeta}|_{\Gamma_0} = \text{arbitrary}, \qquad \bar{\zeta}|_{\Gamma_{D\zeta}} = c, \qquad \left.\frac{\partial \bar{\zeta}}{\partial n}\right|_{\Gamma_{N\zeta}} = d \tag{21b}$$

$$-\nabla^2 \bar{\psi} = \bar{\zeta} \tag{22a}$$

$$\bar{\psi}|_{\Gamma_{D\psi}} = a, \qquad \left.\frac{\partial \bar{\psi}}{\partial n}\right|_{\Gamma_{N\psi}} = b \tag{22b}$$

so that β can be evaluated through the expression

$$\beta(s) = -\int_\Omega (\bar{\zeta} w - \nabla \bar{\psi} \cdot \nabla w) - \int_{\Gamma_0} b_0 w \tag{23}$$

After the linear problem

$$A\lambda = \beta \tag{24}$$

has been solved, the sought solutions to the vorticity equation (10) and to the stream

function equation are obtained from the equations

$$(-\nabla^2 + e)\zeta = f \tag{25a}$$

$$\zeta|_{\Gamma_0} = \bar{\zeta}|_{\Gamma_0} + \lambda, \qquad \zeta|_{\Gamma_{D\zeta}} = c, \qquad \left.\frac{\partial \zeta}{\partial n}\right|_{\Gamma_{N\zeta}} = d \tag{25b}$$

$$-\nabla^2 \psi = \zeta \tag{26a}$$

$$\psi|_{\Gamma_{D\psi}} = a, \qquad \left.\frac{\partial \psi}{\partial n}\right|_{\Gamma_{N\psi}} = b \tag{26b}$$

WEAK FORM OF THE EQUATIONS

Let $H^1(\Omega)$ be the standard Sobolev space of scalar functions defined on Ω which are square integrable together with their first-order derivatives. Furthermore, let $H^1_{\Gamma^*}(\Omega)$ be the space of functions $\varphi \in H^1(\Omega)$ which vanish on the part Γ^* of the boundary Γ of Ω, i.e. such that $\varphi|_{\Gamma^*} = 0$. In addition, (φ, φ') indicates the Hilbert scalar product in the space $L^2(\Omega)$ and $(\boldsymbol{\varphi}, \boldsymbol{\varphi}')$ denotes the scalar product in the space $(L^2(\Omega))^2$ of square integrable vector functions with two components. By means of standard methods, we can restate problems (18) and (19) in a variational form as follows: for each $s' \in \Gamma_0$, find $\zeta' \in H^1(\Omega)$ such that

$$(\nabla \zeta', \nabla \varphi) + e(\zeta', \varphi) = 0, \qquad \forall \varphi \in H^1_{\Gamma_0 \cup \Gamma_{D\zeta}}(\Omega) \tag{27a}$$

$$\zeta'|_{\Gamma_0} = \delta(s - s'), \qquad s \in \Gamma_0, \qquad \zeta'|_{\Gamma_{D\zeta}} = 0 \tag{27b}$$

and $\psi' \in H^1(\Omega)$ such that

$$(\nabla \psi', \nabla \varphi) = (\zeta', \varphi), \qquad \forall \varphi \in H^1_{\Gamma_{D\psi}}(\Omega) \tag{28a}$$

$$\psi'|_{\Gamma_{D\psi}} = 0 \tag{28b}$$

respectively. In a similar way, problems (21) and (22) become: given f, c, and d, find $\bar{\zeta} \in H^1(\Omega)$ such that

$$(\nabla \bar{\zeta}, \nabla \varphi) + e(\bar{\zeta}, \varphi) = (f, \varphi) + \int_{\Gamma_{N\zeta}} \varphi d, \qquad \forall \varphi \in H^1_{\Gamma_0 \cup \Gamma_{D\zeta}}(\Omega) \tag{29a}$$

$$\bar{\zeta}|_{\Gamma_0} = \text{arbitrary}, \qquad \bar{\zeta}|_{\Gamma_{D\zeta}} = c \tag{29b}$$

and, given $\bar{\zeta}$, a and b, find $\bar{\psi} \in H^1(\Omega)$ such that

$$(\nabla \bar{\psi}, \nabla \varphi) = (\bar{\zeta}, \varphi) + \int_{\Gamma_{N\psi}} b\varphi, \qquad \forall \varphi \in H^1_{\Gamma_{D\psi}}(\Omega) \tag{30a}$$

$$\bar{\psi}|_{\Gamma_{D\psi}} = a \tag{30b}$$

Using the scalar product notation, equations (20) and (23) read

$$A(s, s') = (\zeta', w) - (\nabla \psi', \nabla w) \tag{31}$$

and

$$\beta(s) = -(\bar{\zeta}, w) + (\nabla \bar{\psi}, \nabla w) - \int_{\Gamma_0} b_0 w \tag{32}$$

respectively. The weak form of problems (25) and (26) can be obtained similarly.

The discretized form of the weak problems considered so far can be obtained by standard methods by replacing the space $H^1(\Omega)$ with some finite dimensional counterpart. A spatial

discretization based on quadrilateral finite elements of Lagrangian type is considered for the numerical application of the present formulation.

EFFECT OF SPATIAL DISCRETIZATION

As a viable means of investigating the effect of the spatial discretization process and comparing the FE and FD approximations, we study the following linearized one-dimensional model problem

$$\frac{\partial \zeta}{\partial t} + w\frac{\partial \psi}{\partial x} - \gamma\frac{\partial^2 \zeta}{\partial x^2} = 0 \tag{33}$$

$$-\frac{\partial^2 \psi}{\partial x^2} = \zeta \tag{34}$$

w and γ being arbitrary constants. For a uniform mesh of piecewise linear finite elements of size h, the standard Galerkin method provides the following semi-discrete equations for the nodal values $\zeta_j(t)$ and $\psi_j(t)$, $j = \ldots 0, 1, \ldots$

$$(1+\rho D)\dot{\zeta}_j + \frac{w}{h}A\psi_j - \frac{\gamma}{h^2}D\zeta_j = 0 \tag{35}$$

$$-\frac{1}{h^2}D\psi_j = \zeta_j \tag{36}$$

where $\rho = \frac{1}{6}$, the upper dot denotes time derivative, $Au_j \equiv (u_{j+1} - u_{j-1})/2$ and $Du_j \equiv u_{j+1} - 2u_j + u_{j-1}$. For $\rho = 0$ equations (35) and (36) also provide the standard finite difference approximation to equations (33) and (34). Assuming an initial condition of the form $\zeta(x, t = 0) = \hat{\zeta}e^{ikx}$, the exact solution of the continuum problem is found to be $\zeta(x, t) = \hat{\zeta}e^{ikx - \lambda t}$, $\psi = \zeta/k^2$ where $\lambda \equiv \delta + i\omega = \gamma k^2 + iw/k$. Furthermore, the exact solution of the semi-discrete problem is of the form

$$\zeta_j(t) = \bar{\zeta}(t)e^{ikjh}, \qquad \psi_j(t) = \bar{\psi}(t)e^{ikjh} \tag{37}$$

By substituting equations (37) into equations (35) and (36) and eliminating $\bar{\psi}$ in favour of $\bar{\zeta}$, we obtain the following single ordinary differential equation for $\bar{\zeta}(t)$

$$[1 + 2\rho(\cos\xi - 1)]\dot{\bar{\zeta}} + iwh\frac{\sin\xi}{2(\cos\xi - 1)}\bar{\zeta} - \frac{\gamma}{h^2}2(\cos\xi - 1)\bar{\zeta} = 0 \tag{38}$$

where $\xi = kh$ is the dimensionless wave number. The solution of equation (38) is of the form

$$\bar{\zeta}(t) = \bar{\zeta}_0 e^{-\bar{\lambda}t} \tag{39}$$

$\bar{\zeta}_0$ being an arbitrary constant (the initial amplitude of the wave) and $\bar{\lambda}$ the semi-discrete response complex variable

$$\bar{\lambda} = \bar{\delta} + i\bar{\omega} \tag{40}$$

$\bar{\delta}$ and $\bar{\omega}$ are given in terms of their continuum counterparts δ and ω, by

$$\frac{\bar{\delta}}{\delta} = \frac{2(1-\cos\xi)/\xi^2}{1 - 2\rho(1-\cos\xi)} \tag{41}$$

$$\frac{\bar{\omega}}{\omega} = \frac{\xi\sin\xi/[2(1-\cos\xi)]}{1 - 2\rho(1-\cos\xi)} \tag{42}$$

By analysing the dependence of the damping ratio $\bar{\delta}/\delta$ and of the frequency ratio $\bar{\omega}/\omega$ versus ξ, it is possible to assess the influence of the spatial discretization on the attenuation and propagation of signals of different wavelengths.

For the case of pure diffusion ($w = \bar{\omega} \equiv 0$), Figure 1(a) shows that the effect of the FE discretization is to increase the damping with respect to exact value at intermediate and short wavelengths. On the contrary, finite differences are seen to reduce the damping particularly in the range of high spatial frequencies.

In the case of pure advection ($\gamma = \bar{\delta} \equiv 0$), Figure 1(b) shows that for wavelengths of practical interest the finite elements produce an increase of the speed of propagation whereas the finite differences have an opposite effect of about the same magnitude. This result is somewhat unexpected because it contrasts with the well known results for the 'standard' advection equation $\zeta_t + v\zeta_x = 0$ (v = a constant) shown in Figure 1(c). In this case both discretizations decrease the propagation speed, the FE approximation being clearly superior.[16] In the mixed case of advection and diffusion, it results that $\bar{\lambda}_{AD} = \bar{\delta} + i\bar{\omega}$ so that the following picture emerges for the coupled ζ–ψ equations. Intermediate wavelengths are propagated at a higher speed and are overdamped by FEs whereas they are propagated

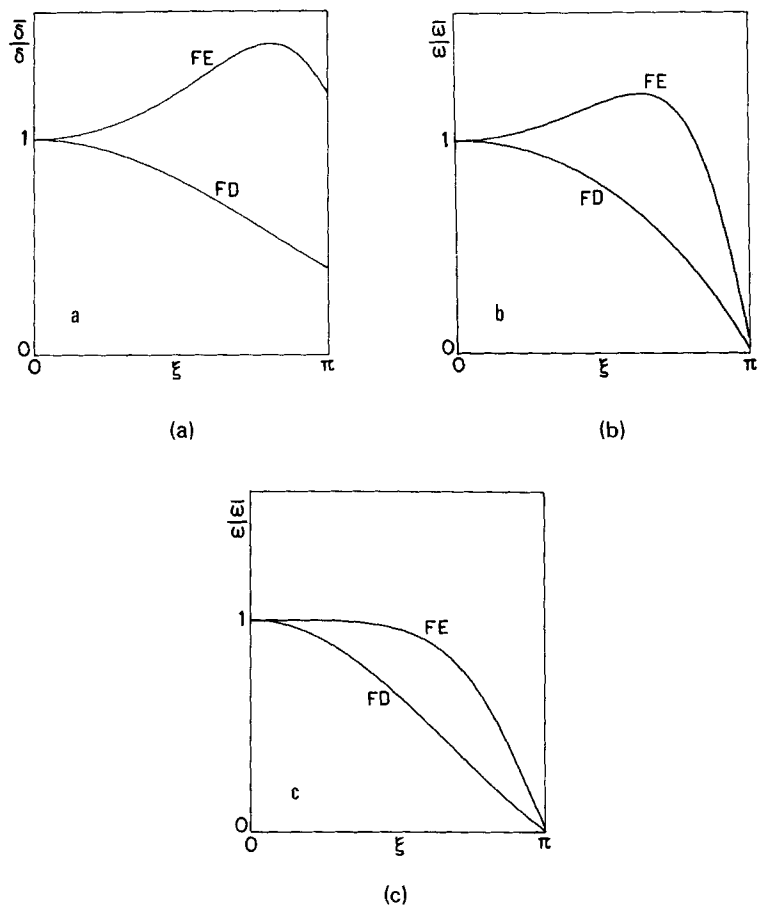

Figure 1. Comparison of finite element and finite difference spatial discretizations of one-dimensional model equations. Semi-discrete response parameters versus the dimensionless wavenumber ξ: (a) diffusion equation; (b) advection equation; (c) standard advection equation

slower and are underdamped by FDs. On the other hand, high spatial frequencies have a lower speed in both discretizations but this misrepresentation is still attenuated by FE whereas it is enhanced by FD.

Furthermore, by writing the advection term (coupling the two equations) in the non-linear form $\zeta_x\psi_x$, we can compare finite elements and finite differences also with respect to the approximation of the fully non-linear equations. The application of the standard Galerkin method to the term $\zeta_x\psi_x$ provides at the node j

$$\frac{1}{2h^2}[(\zeta_{j+1}-\zeta_j)(\psi_{j+1}-\psi_j)+(\zeta_j-\zeta_{j-1})(\psi_j-\psi_{j-1})]$$

which is a centred approximation averaged on two neighbouring elements. Instead, the standard finite difference approximation of $\zeta_x\psi_x$ is

$$\frac{1}{4h^2}(\zeta_{j+1}-\zeta_{j-1})(\psi_{j+1}-\psi_{j-1})$$

i.e. the usual second-order discretization. The superiority of the Galerkin FE method over the standard FD one is evident.

Thus, the FE discretization is expected to be globally superior. This has been confirmed by the numerical solutions of the full vorticity–stream function equations to be presented in the next section.

NUMERICAL EXAMPLES AND COMPARISONS

All the computations presented in this section have been performed using single-precision arithmetic (IBM 370-165) except for double-precision accumulation of scalar products in the LLT factorization of the banded or full symmetric matrices. The convergence criteria used in all of the following numerical examples are based on the *infinite* norm, i.e. $\|\varphi\| \equiv \max\{\varphi_i\}$ and $\|(\zeta, \psi)\| \equiv \max\{\|\zeta\|, \|\psi\|\}$.

First, the classical driven cavity problem[17] has been considered, for which a one-to-one comparison with the results obtained by the equivalent method using finite differences[14] is possible. Transient as well as steady-state results are presented, the unsteady flow problem being impulsively started from rest. Table II gives the number of time steps n and of total iterations m necessary to reach the steady state for $Re = 100$ and two different values of the time step $\Delta t = 0{\cdot}1$ and $\Delta t = 1$. Three spatial discretizations are considered: FD, a hybrid FD–FE approximation[14] and the finite element approximation using isoparametric 4-noded quadrilateral elements with all integrals evaluated numerically by the 2×2 Gauss product formula. The hybrid approximation is basically an FD discretization with the Jacobian evaluated according to the Arakawa's second-order nine-point differencing[18] which is known to be equivalent to a Galerkin approximation using bilinear finite elements. From Table II it appears that all spatial discretizations and all time integration schemes are equally reliable for the smaller value of Δt, the FD method seeming slightly more rapid in achieving the steady state. On the contrary, for the larger value of Δt, the trend reverses and actually the explicit and implicit FD schemes definitely have some difficulty in accurately modelling the transient. In addition, the hybrid method is found to have an intermediate behaviour, as expected. We have numerically evaluated the total vorticity $\int d\Omega\zeta$ from some of the finite element solutions at some selected times. This quantity is physically important, being related

Table II. Time dependent driven cavity problem. Number of time steps n and of total iterations m necessary to reach the steady state within $\sigma = 10^{-3}$. $Re = 100$, $\varepsilon = 10^{-3}$, uniform mesh 8×8, $\Delta t = 0{\cdot}1$ (upper part) and $\Delta t = 1$ (lower part)

	FE		Hybrid		FD	
Time integration scheme	n	m	n	m	n	m
Explicit	93	—	82	—	73	—
ζ-implicit	92	272	80	193	73	189
ψ-implicit	94	121	83	104	75	92
Implicit	92	290	83	218	74	211
Explicit	21	—	17	—	75	—
ζ-implicit	12	117	14	62	17	92
ψ-implicit	20	44	16	34	41	58
Implicit	17	120	16	80	15	175

to the basic conservation law[8]

$$\int d\Omega\zeta = -\int d\Gamma \frac{\partial\psi}{\partial n}$$

that follows directly from the equation $-\nabla^2\psi = \zeta$. This law can be regarded as the vorticity integral condition with respect to the trivial harmonic function $\eta \equiv 1$. In the driven cavity problem, $\partial\psi/\partial n = 0$ except on the upper wall where $\partial\psi/\partial n = 1$, so that $\int d\Omega\zeta = -1$. In all cases it has been found $\int d\Omega = -1$ with an accuracy of seven significant decimal digits in our single-precision calculations.

In order to assess the accuracy of the proposed method, the profile of the horizontal velocity u_x along the vertical centreline of the cavity for $Re = 100$ at various times and at the steady state, obtained with a uniform mesh of 16×16 elements, is compared with the corresponding results obtained with the FD method employing standard second-order centred differences on the meshes 16×16 and 32×32. The results given in Figure 2 clearly indicate the superior accuracy of the FE spatial discretization. In Table III we report the stream function value at, and the position of, the centre of the main vortex for $Re = 100$ at $t = 0{\cdot}5$, 1, 1·5 and 2. The transient is modelled by the FE method in fair agreement with the FD solution calculated using a twice finer mesh. For completeness, the vorticity contours and the streamlines at the same times are presented in Figure 3.

In order to investigate the robustness of the method, the case $Re = 1000$ has been attempted with the rather coarse uniform mesh 16×16. In contrast with the second-order accurate FD approach which was never able to converge on this mesh, the present FE method is capable of providing a transient solution which is depicted in Figure 4. In spite of visible vorticity oscillations near the driving wall, the overall accuracy of this solution is quite adequate. For instance, the maximum value of the stream function $\psi = -0{\cdot}0615$ and $\psi = -0.0759$ at $t = 5$ and $t = 10$, respectively, are very near to the FD values $\psi = -0{\cdot}060$ and $\psi = -0{\cdot}0738$ obtained using a fourth-order accurate discretization of the advection term and a uniform mesh 32×32. An analogous agreement is found for the position of the centre of the main vortex. The vorticity oscillations in the first three rows of nodes near the driving

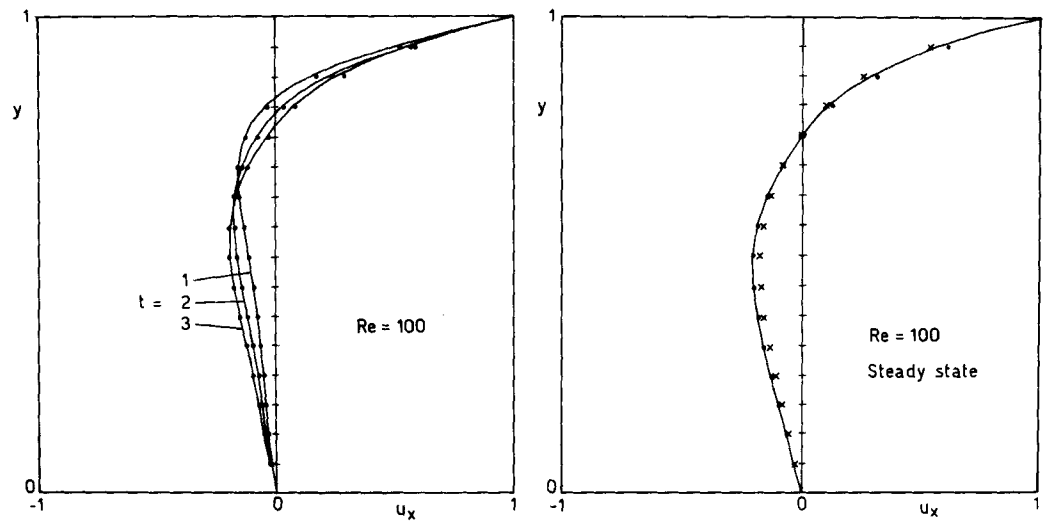

Figure 2. Horizontal velocity along the vertical centreline in the driven cavity problem: $Re = 100$; ● finite elements 16×16; × finite differences 16×16; —— finite differences 32×32

wall using the uniform mesh are detailed in Figure 5(a). Node-to-node oscillations are present both in the x-direction and in the y-direction. Notice that at the first row of internal nodes there is an even/odd separation of the vorticity values similar to the one predicted by Gresho and Lee[19] for the steady-state solution to the (standard) advection–diffusion equation using an even number of equal linear elements: the even node values match the boundary values at both extremes, whereas the odd node values do not. In Figure 5(b) we show how the vorticity oscillations are reduced by using a non-uniform mesh.

Finally, in order to verify the formulation in the presence of boundary conditions for the vorticity, we have considered the channel flow problem proposed by Roache.[20]

The geometry, the finite element mesh and the boundary conditions are given in Figure 6 for the case $Re = 10$. The steady-state vorticity along the lower wall obtained by the implicit scheme of the present formulation is given in Figure 7. The present numerical solution is found to be remarkably close to the one obtained by a fourth-order accurate spline ADI technique,[21] using the same mesh. For instance, the separation bubble centre is located at the same grid point $x = 1{\cdot}130$, $y = -0{\cdot}6645$ and the corresponding value of the stream function is $\psi = -0{\cdot}0011$ for both methods.

Table III. Main vortex strength and position versus time. $Re = 100$, ψ-implicit scheme, $\varepsilon = 10^{-3}$, uniform mesh

	FE: 16×16			FD: 32×32		
t	ψ_{vc}	x_{vc}	y_{vc}	ψ_{vc}	x_{vc}	y_{vc}
0·5	−0·0565	0·6875	0·875	−0·0551	0·6875	0·875
1·0	−0·0730	0·6875	0·8125	−0·0714	0·65625	0·8125
1·5	−0·0828	0·6875	0·8125	−0·0812	0·65625	0·8125
2·0	−0·0883	0·6875	0·8125	−0.0871	0·65625	0·78125

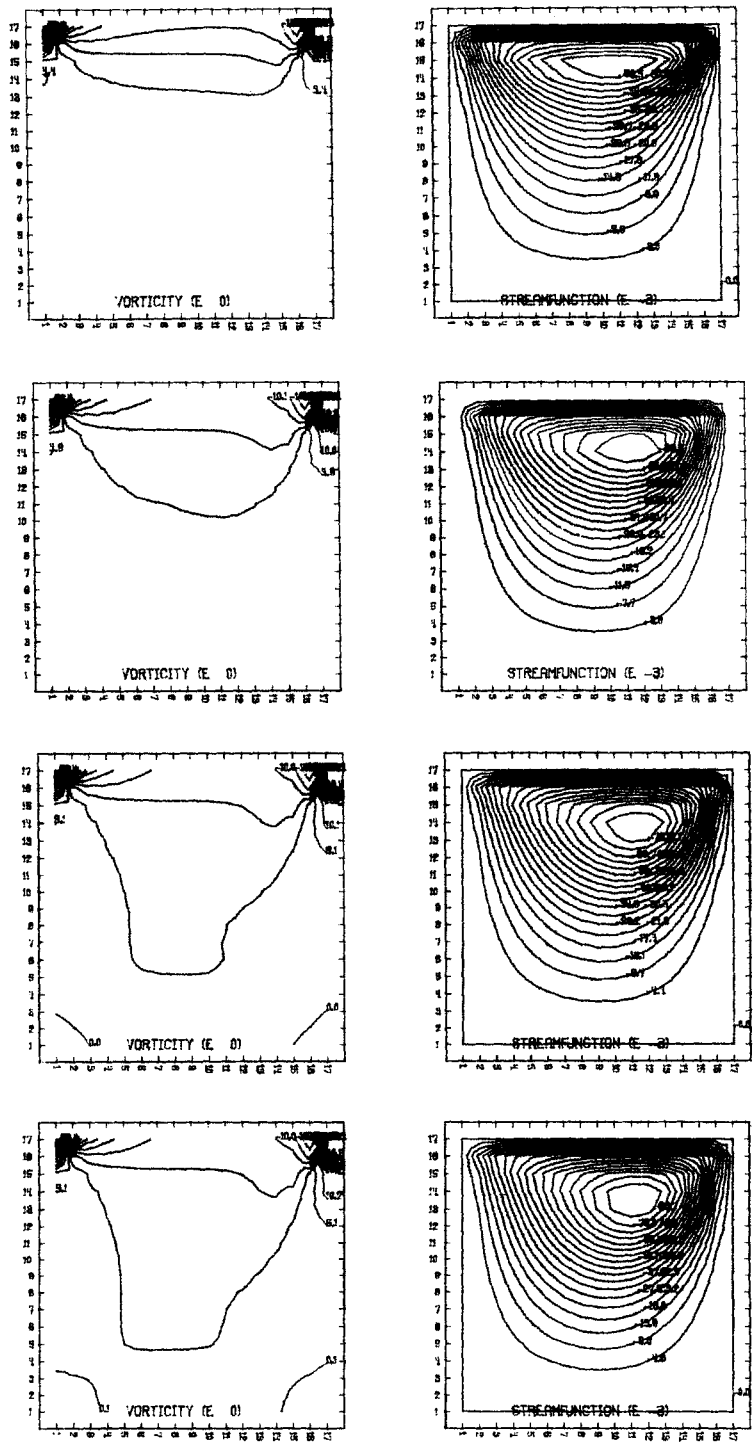

Figure 3. Impulsively started flow in a square cavity at $t = 0{\cdot}5$, 1, $1{\cdot}5$ and 2: $Re = 100$, ψ-implicit scheme, $\Delta t = 0{\cdot}05$, uniform mesh 16×16

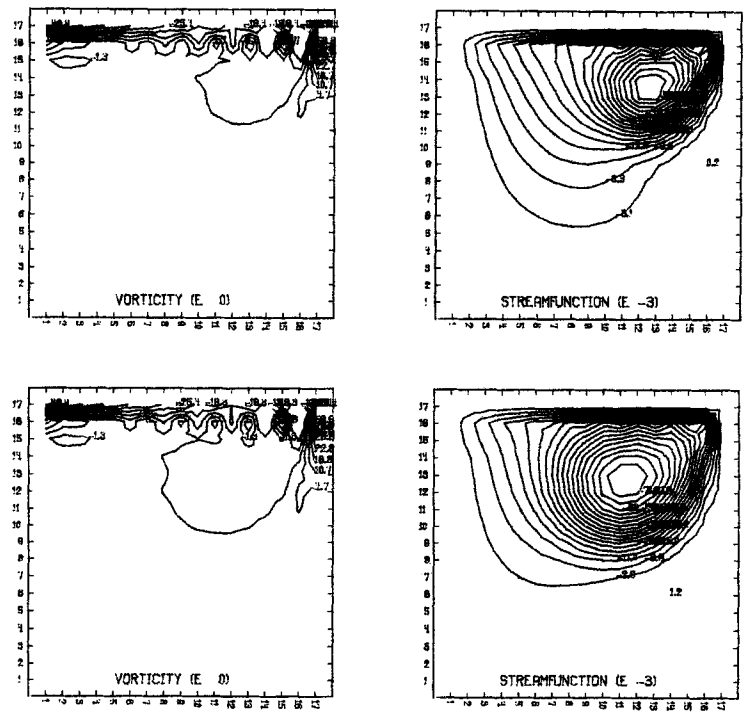

Figure 4. Impulsively started flow in a square cavity at $t = 5$ and $t = 10$: $Re = 1000$, ψ-implicit scheme, $\Delta t = 0{\cdot}05$, uniform mesh 16×16

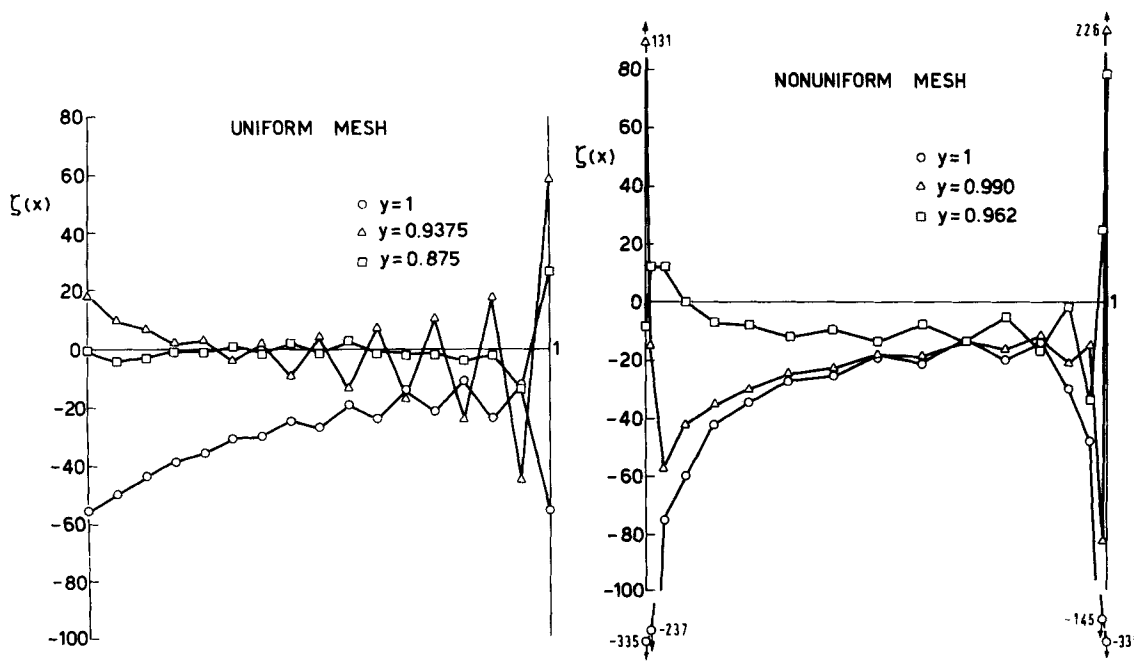

Figure 5. Vorticity profiles at, and near to, the driving wall in the impulsively started flow in a square cavity. $Re = 1000$, $t = 5$, ψ-implicit scheme, $\Delta t = 0{\cdot}05$, uniform mesh (left) and non-uniform mesh (right) 16×16

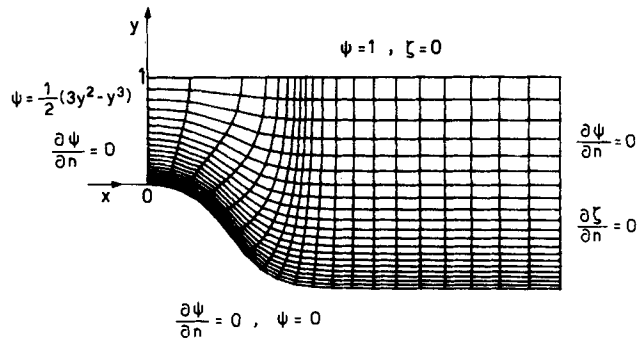

Figure 6. Channel flow geometry, mesh and boundary conditions for $Re = 10$

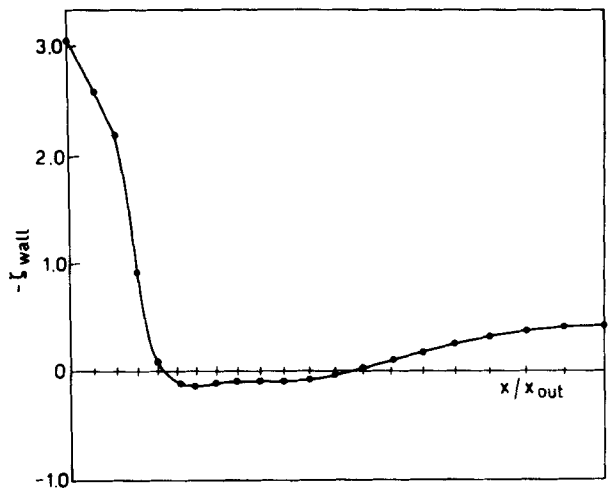

Figure 7. Wall vorticity of the channel flow problem for $Re = 10$ at the steady state within $\sigma = 10^{-3}$. Implicit scheme, $\varepsilon = 10^{-3}$, $\Delta t = 0{\cdot}1$, $n = 63$ and $m = 203$

CONCLUSIONS

A finite element method for calculating two-dimensional incompressible viscous flows has been presented in which the unsteady vorticity-stream function equations are solved as a cascade of elliptic (Helmholtz and Poisson) problems. This has been made possible by means of integral conditions for the vorticity allowing a splitting of the Navier–Stokes equations. The robustness and validity of the present formulation have been demonstrated by a few numerical examples which have shown the superiority of the spatial discretization by bilinear finite elements over FD discretizations of the same order of accuracy. The present method can be easily extended to axisymmetric flows[13] and to natural convection problems.

ACKNOWLEDGEMENTS

The authors are indebted to Jean-Pierre Halleux who made this work possible and to Cornelis L. van den Muyzenberg for his guidance in the design and implementation of the

finite element algorithm. The computer program (language PL/I) can be obtained from the authors upon request.

REFERENCES

1. H. B. Keller and H. Takami, in D. Greenspan (ed.) *Numerical Solutions of Nonlinear Differential Equations*, Prentice-Hall, Englewood Cliffs, New Jersey, 1966.
2. J. W. McLaurin, *SIAM J. Num. Anal.*, **11,** 14–33 (1974).
3. P. J. Roache, *Computational Fluid Dynamics*, 2nd edn., Hermosa Publishers, Albuquerque, 1976.
4. S. A. Orszag and M. Israeli, *Ann. Rev. Fluid Mech.*, **6,** 281–318 (1974).
5. S. L. Smith and C. A. Brebbia, *J. Comp. Phys.*, **17,** 235–245 (1975).
6. M. D. Olson in *Proc. Mc Gill-EIC Conf. on FEM in Civil Engg.*, Montreal, 1972.
7. J. H. Argyris and G. Mareczek, *Ing. Arch.*, **43,** 92–109 (1974).
8. G. J. Fix, *SIAM Review*, **18,** 460–480 (1976).
9. A. Campion-Renson and M. J. Crochet, *Int. J. Num. Meth. Eng.*, **12,** 1809–1818 (1978).
10. O. Axelsson and I. Gustafsson, *Comp. Meth. Appl. Mech. Eng.*, **20,** 9–16 (1979).
11. M. Fortin and F. Thomasset, *J. Comp. Phys.*, **31,** 113–145 (1979).
12. S. C. R. Dennis and S. N. Singh, *J. Comp. Phys.*, **28,** 297–314 (1978).
13. L. Quartapelle and F. Valz-Gris, *Int. j. numer. methods fluids*, **1,** 129–140 (1981).
14. L. Quartapelle, *J. Comp. Phys.*, **40,** 453–477 (1981).
15. R. Glowinski and O. Pironneau, *SIAM Review*, **21,** 167–212 (1979).
16. P. M. Gresho, R. L. Lee and R. L. Sani, in *Finite Elements in Fluids*, Vol. 3, Wiley, New York, 1978.
17. O. Burggraf, *J. Fluid Mech.*, **24,** 113–151 (1966).
18. A. Arakawa, *J. Comp. Phys.*, **1,** 119–143 (1966).
19. P. M. Gresho and R. L. Lee, in T. J. R. Hughes (ed.) *Finite Element Methods for Convection Dominated Flows*, AMD, Vol. 34, New York, 1979.
20. P. J. Roache, 'Scaling of high Reynolds number weakly separated channel flows', *Symposium on Numerical and Physical Aspects of Aerodynamic Flows*, 19–21 January 1981, California State University, Long Beach, California.
21. M. Napolitano, 'Efficient ADI and spline ADI methods for the Navier–Stokes equations', AFWAL-TR, 1982, to appear.